THE JOURNAL OF PHYSICAL CHEMISTRY Letters

pubs.acs.org/JPCL

Definitive Band Gaps for Single-Wall Carbon Nanotubes

Yuki Matsuda, Jamil Tahir-Kheli, and William A. Goddard, III*

Materials and Process Simulation Center, California Institute of Technology, California 91125

ABSTRACT We report ab initio quantum mechanical calculations of band structures of single-walled carbon nanotubes (SWNTs) using the B3LYP flavor of density functional theory. In particular, we find excellent agreement with the small band gaps in "metallic" zigzag SWNTs observed by Lieber et al. [0.079 vs 0.080 eV for (9,0), 0.041 vs 0.042 eV for (12,0), and 0.036 eV vs 0.029 eV for (15,0)]. This contrasts with the results from LDA and PBE, which lead to band gaps 70−100% too small, and with those from the GW correction to LDA, which leads to a gap two times too large. Interestingly we find that the (5,0) system, expected to be a large gap semiconductor, is metallic. These results show that B3LYP leads to very accurate band gaps for CNTs, suggesting its use in designing CNT devices. We find that the effective mass of the CNT (significant in designing CNT devices) scales inversely proportional to the square of the diameter.

SECTION Electron Transport, Optical and Electronic Devices, Hard Matter

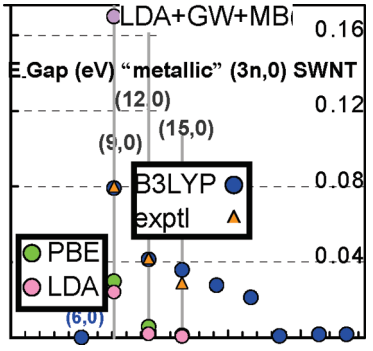

Carbon nanotubes (CNTs) provide a number of unique and special properties that suggest great promise for nanoelectronics applications. In particular, the high electrical conductivity of quantum wires provides a potential solution for on-chip interconnect metals and transistors of future integrated circuits.

One crucial obstacle to overcome in fabrication is controlling whether the CNT is metallic or semiconducting. The critical parameter determining the electronic properties of CNTs is the chiral vector, $C_h = (na_1 + ma_2) \equiv (n,m)$, where n and m are integers and a_1 and a_2 are the real space unit vectors of the graphene sheet. C_k specifies the way the graphene sheet is wrapped. When $n - m$ is a multiple of 3, the simple theory leads to a crossing of bands at the Fermi energy, implying that CNT is metallic; otherwise, it is expected to be a semiconductor. Thus, armchair (n,n) CNTs are expected to always be metallic, whereas zigzag $(n,0)$ CNTs are expected to be metallic only when n is a multiple of 3.

However, on the basis of measurements under ultrahigh vacuum conditions at 5 K on a Au(111) substrate, Lieber et al.[1] showed that some $(3m,0)$ zigzag single-walled carbon nanotubes (SWNTs) have finite band gaps [0.080 ± 0.005 eV for (9,0), 0.042 ± 0.004 eV for (12,0), and 0.029 ± 0.004 eV for (15,0)].

Previous quantum mechanical (QM) calculations were not able to account for the observed band gaps.[2,3] The local density approximation (LDA) functional in density functional theory (DFT) led to gaps of 0.024 eV for (9,0), 0.002 eV for (12,0), and 0 eV for (15,0), which are 70, 95, and 100% too small. Of course, it is well-known that LDA leads to band gaps that are too small. A common approach to correcting these LDA band gaps is the GW approximation, which calculates the poles of the Green's functions explicitly. For (9,0), GW leads to a band gap that is too large by 213%.[2] The generalized gradient approximation (GGA) functional leads to much more accurate cohesive energies than LDA, but the Perdew−Burke−Ernzerhof (PBE) flavor leads to band gaps of 0.030 eV for (9,0), 0.010 eV for (12,0), and 0 eV for (15,0), which are 63, 86, and 100% too small. The Perdew−Wang 91 (PW91) flavor of GGA corrected with an empirical uniform scale factor (1.20) leads[3] to band gaps of 0.20 eV for (9,0), 0.08 eV for (12,0), and 0.14 eV for (15,0), which are to large by 250, 190, and 483% of the experimental values, respectively, following no consistent trend.

Since the band gap is the most significant property in designing CNTs for electronics applications, it is essential to find a way of predicting accurate band gaps. We report such an approach here.

The problem with bad band gaps from DFT calculations has been encountered before. A spectacular case is for the undoped parent compound, La_2CuO_4, of cuprate superconductors,[4] where LDA and GGA lead to highly overlapping bands at the Fermi energy and hence a metal, whereas this system has an experimental band gap of 2.0 eV. Perry et al.[4] solved this problem by showing that the Becke−Lee−Yang−Parr (B3LYP) flavor[5] of DFT leads to an accurate band gap of 2.0 eV. Indeed, similar results have now been reported for many other semiconductor and insulator systems.[6] The B3LYP functional combines the Becke GGA exchange potential based with Hartree−Fock (HF) exact exchange plus the Lee−Yang−Parr correlation functional.[5] B3LYP has been shown to provide the most accurate cohesive energies, ionization potentials, and electron affinities for a range of finite molecules.[7,8] The inclusion of exact HF exchange helps to correct for the self-energy problem with standard DFT formulations.

Received Date: June 30, 2010
Accepted Date: September 14, 2010
Published on Web Date: September 20, 2010

DOI: 10.1021/jz100889u | J. Phys. Chem. Lett. 2010, 1, 2946–2950

On the basis of these successes, we decided to apply B3LYP to the problem of CNT band gaps. Indeed, we find that the B3LYP flavor of density functional[5] theory leads to accurate band gaps of these zigzag SWNTs with values of 0.079 eV for (9,0), 0.041 eV for (12,0), and 0.036 eV for (15,0). These are within 0.001, 0.001, and 0.007 eV of the experimental values, respectively, a spectacular agreement. This excellent agreement for the most challenging case of the nonmetallic (3*m*,0) zigzag CNTs validates the use of B3LYP to predict the band gaps and other properties of CNT systems.

Our studies of other (*n*,0) zigzag CNTs find that both (6,0) and (24,0) are metallic, even though the (9,0), (12,0), and (15,0) systems are semiconducting. Experiments on these systems would be useful to provide additional validation of our results.

Since B3LYP does so well for energy gaps, we anticipate that it should be accurate for other properties such as effective masses and the Fermi velocity needed for designing nanoelectronic devices, and we report such values here.

Tests against Diamond and Graphite. As a preliminary test of B3LYP, we calculated the band structures of diamond and graphite. Table 1 and Figure S1 (see Supporting Information) compare critical energies from B3LYP with experimental data[9−11] and the results from LDA and PBE.

For diamond, B3LYP leads to an indirect band gap of 5.5 eV compared to 5.5 eV from experiment.[9] PBE and LDA obtain 3.9 and 3.3 eV, respectively. Similarly, the direct band gap at Γ from B3LYP is 7.2 eV, compared to 7.3 eV from experiment[10] while PBE and LDA values are 5.5 and 5.3 eV.

Table 1. Band Gap (eV) of Diamond and Graphite Using Various Functionals (LDA, PBE, and B3LYP) Compared with Experimental Gaps

		LDA	PBE	B3LYP	experiment
diamond	indirect	3.3	3.9	5.5	5.5[a]
	Γ	5.3	5.5	7.2	7.3[b]
graphite	Γ[c]	11.0	11.4	13.6	∼13.1[d]

[a] Reference 9. [b] Reference 10. [c] $\sigma-\sigma^*$ transition. [d] Reference 11.

For graphite, the valence and conduction bands touch at the K point, leading to a semimetal. The direct band gap at Γ from B3LYP is 13.6 eV, compared to ∼13.1 eV from experiment.[11] PBE is 11.0 eV, and LDA is 11.4 eV.

It has recently been shown[12] that the inclusion of exact Hartree−Fock exchange compensates for the error of fractional electron occupations. This may be the reason for the success of B3LYP for CNTs reported here.

(*3m,0*) *"Metallic" Zigzag SWNT.* Figure 1b shows that the small band gaps found experimentally[1] for the (9,0), (12,0), and (15,0) cases of metallic (3*m*,0) zigzag SWNTs are in excellent agreement with the values calculated from B3LYP (Table 2). These computed band gaps scale as $\sim 1/d^2$, a trend that continues for (18,0) and (21,0). However, for (6,0) and beyond (24,0), we find no band gap ($E_g = 0$). These trends

Table 2. Band Gaps (E_g) of Metallic ($(n-m)/3$ = integer) Zigzag and Chiral SWNTs for B3LYP, PBE, and LDA Compared to Experiment

n[a]	m[a]	diameter (nm)[b]	B3LYP E_g (eV)	experimental E_g (eV)	PBE E_g (eV)	LDA E_g (eV)
6	0	0.489	0.00			
9	0	0.713	0.079	0.080 ± 0.005[c]	0.003	0.024
12	0	0.951	0.041	0.042 ± 0.004[c]	0.006	0.002
15	0	1.182	0.036	0.029 ± 0.004[c]	0.00	0.00
18	0	1.420	0.028			
21	0	1.655	0.021			
24	0	1.855	0.00			
27	0	2.217	0.00			
30	0	2.317	0.00			
5	5	0.557	0.00			
10	10	1.366	0.00	0.00[c]		
8	2	0.725	0.00			
11	5	1.121	0.00			
16	4	1.446	0.00			
15	6	1.478	0.00			

[a] Chiral vectors, $C_h = (n,m)$ [b] After optimizations. [c] Reference 1.

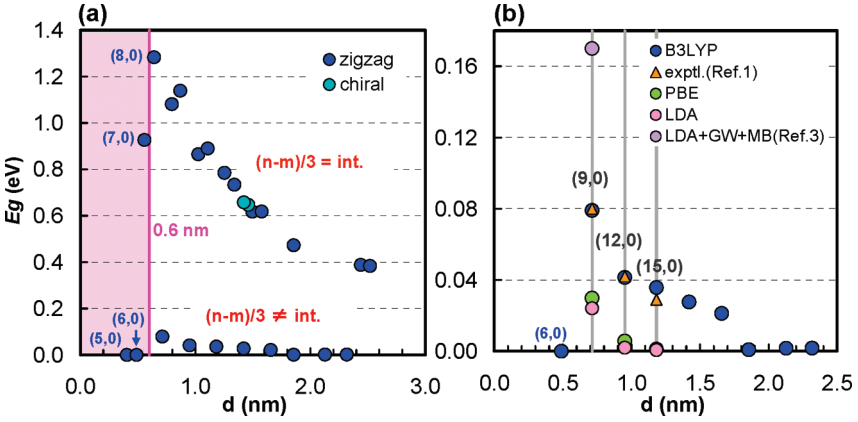

Figure 1. (a) Band gaps of zigzag SWNTs (dark blue circles) calculated by B3LYP as a function of diameter. Chiral SWNTs (light blue circles), (15,5) of $d = 1.42$ nm and (14,7) of $d = 1.46$ nm, are also plotted. (b) Band gaps of metallic zigzag (3*m*,0) SWNTs as a function of diameter. B3LYP (blue circles), experimental (orange triangles), PBE (yellow green circles), LDA (pink circles), LDA + GW approximation + many-body effects[3] (violet circles).

DOI: 10.1021/jz100889u | J. Phys. Chem. Lett. 2010, 1, 2946–2950

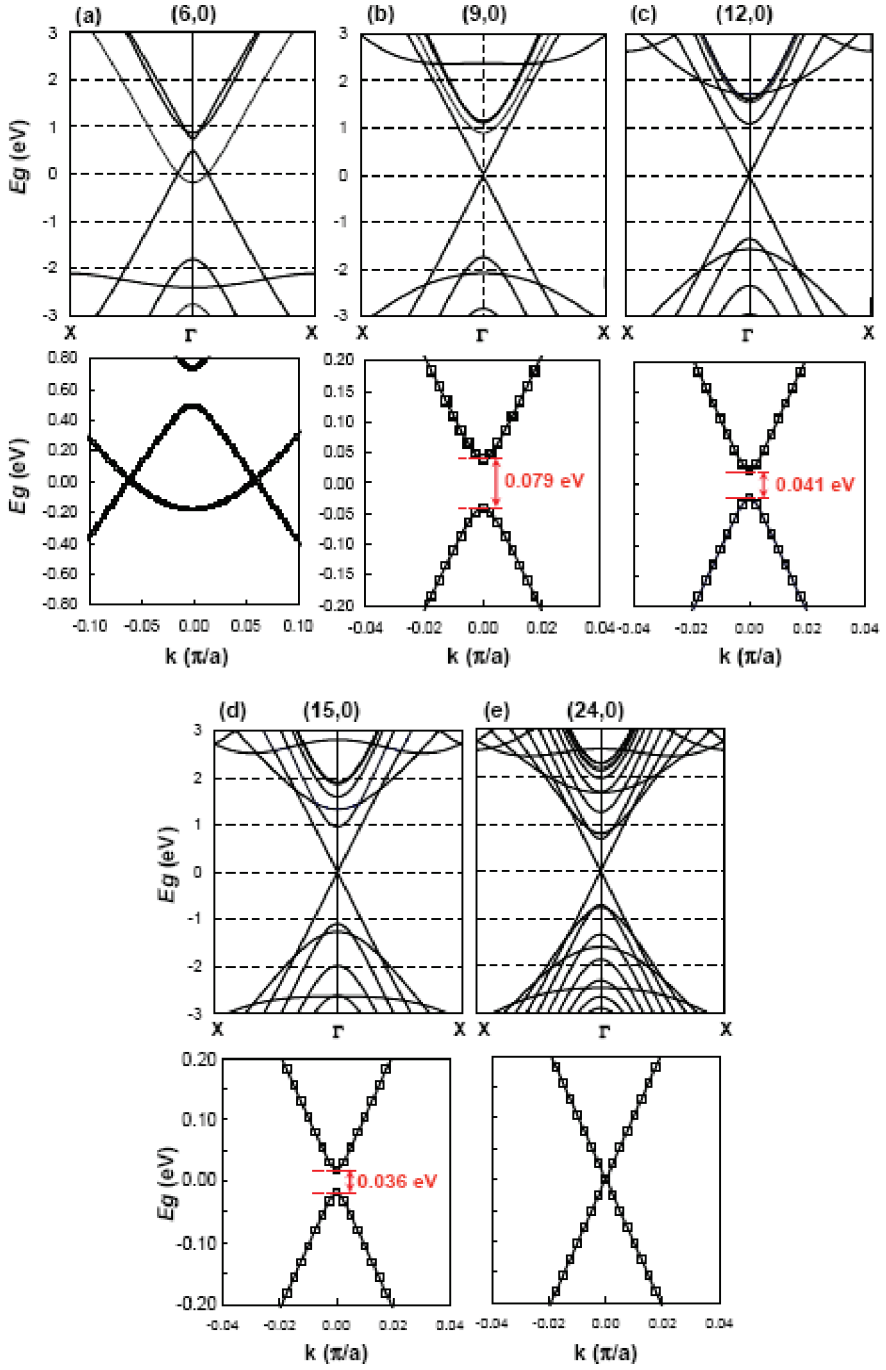

Figure 2. B3LYP band structures of zigzag SWNTs (top) with enlarged scale near the Fermi energy (bottom). (a) (6,0), (b) (9,0), (c) (12,0), (d) (15,0), and (e) (24,0) The small gaps are in good agreement with the experimental data by Lieber et al. (Table S1 in Supporting Information).[1]

can be understood in Figure 2, which shows the $\pi-\pi^*$ coupling near the expected crossing points (K points on the Brillouin zone) of these $3n$ zigzag SWNTs.

It has been argued that this finite gap for $(3m,0)$ with m = 3, 4, 5, and 6 might arise due to such effects as distortions from the Au(111) substrate. In fact, we previously studied SWNTs and graphene sheets in contact with various metal surfaces and determined that side contacts with the Au(111) surface leads to negligible interaction.[13] The equilibrium binding energy of Au(111)−graphene is only 0.13 kcal/mol/atom, leading to negligible strain at the Au surface.

Our results imply the small band gaps arise from the intrinsic properties of the SWNTs and are not due to adsorbates or deformations caused by the interactions between the Au surface and SWNTs.

($n \neq 3m,0$) Nonmetallic SWNT. Figure 1a shows the band gaps of SWNTs as a function of diameter. For $d > 0.6$ nm, we find that the zigzag SWNTs $(n,0)$ with n mod 3 $\neq$ 0 are

DOI: 10.1021/jz100889u | J. Phys. Chem. Lett. 2010, 1, 2946–2950

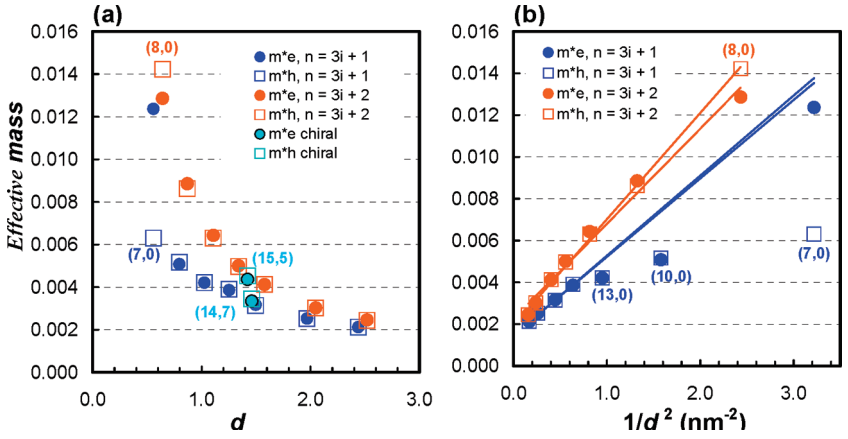

Figure 3. (a) Calculated effective electron (m^*_e) and hole (m^*_h) masses (in units of the electron mass) of semiconductor SWNTs from B3LYP as a function of diameter. (b) Effective masses of zigzag SWNTs scale as the diameter squared. m^*_e is shown in solid circles and m^*_h in open squares (blue, $n = 3i + 1$ (i is integer); orange, $n = 3i + 2$; light blue, chiral).

semiconductors, as expected according to the chiral vector rule, and that the gap increases monotonically with decreasing diameter d until $d < 0.6$ nm, where the gap decreases for (7,0) and is 0 (metallic) for (6,0) and (5,0).

Barone et al.[14] examined LDA, PBE, and B3LYP for a number of nonmetallic cases (but no metallic ones) using the 3-21G basis set. They found that LDA and PBE are systematically lower than B3LYP by ~0.4 eV.

Small Zigzag SWNT: (7,0), (6,0), and (5,0). Figure S3-1a, b, and c (see Supporting Information) shows that the singly degenerate bands at the conduction band minimum (CBM) cross the Fermi energy near the Γ points for (5,0) and (6,0) SWNTs, while it approaches the Fermi energy near the Γ point for the (7,0) SWNT. This is due to the $\sigma^*-\pi^*$ hybridization effects caused by the curvature of small-diameter CNTs.[15] In these small CNTs, the π^* and σ^* states mix and repel each other, leading to lower pure π^* states. The $\sigma^*-\pi^*$ hybridization is not included in common tight-binding (TB) calculations so that TB fails to describe asymmetrical charge transfer of the atoms, leading to finite gaps for (5,0)[16] and (6,0) (e.g., the sp^3s^* TB model[17] leads to $E_g = 0.18$ eV).

Comparisons of Chiral Cases Having the Same Diameter. For the two cases (15,5) and (14,7) that have nearly the same diameter ($d = 1.42$ and 1.46 nm, respectively), we calculate nearly the same band gap $E_g = 0.66$ and 0.65 eV, respectively. This suggests that the band gap of these chiral systems depends mainly on the diameter (i.e., the curvature). The experimental values from Wildöer et al.[18] are $E_g = 0.50-0.60 \pm 0.1$ eV for chiral SWNTs with $d = 1.4 \pm 0.1$ nm.

Effective Masses and Fermi Velocities. Figure 3a shows the calculated effective electron (m^*_e) and hole (m^*_h) masses of semiconductor SWNTs from the B3LYP band structures (in units of the electron mass). We find a different trend for the effective masses of zigzag SWNTs with $n = 3i + 1$ (i is integer) compared to those with $n = 3i + 2$. For (7,0) and (8,0) zigzag SWNTs, the asymmetry of the conduction and valence bands leads to different effective masses of electrons and holes, lending support to the interpretation in terms of $\sigma^*-\pi^*$ hybridization. For larger-diameter SWNTs, the symmetry of the conduction and valence bands ($\pi-\pi^*$) leads to the same effective electron and hole mass. The trend of the effective masses of zigzag SWNTs based on the subgroups $n = 3i + 1$ and $n = 3i + 2$ can be explained by how the allowed k points cross the corner of Brillouin zone. The allowed k points cross closer to the K point for $n = 3i + 2$, leading to effective masses derived from the larger slope in the conduction and valence bands that corresponds to the π orbitals in three dimensions. The masses scale as the diameter squared when $d > 1.0$ nm ($i > 16$ for $n = 3i + 1$ and $i > 11$ for $n = 3i + 2$) (Figure 3b). Since the allowed k points cross closer to the K points with larger diameters, the effective masses and band gaps decrease.

Computational Methodology. The structures for all systems were obtained using the graphite force field[19] that accurately predicts structures and cohesive energies of fullerenes molecules, CNTs, and graphitic crystals.[20,21] The CNT geometries were fully optimized with no symmetry constraints. Detailed structural parameters are given in Table S1 in the Supporting Information.

For the band calculations, we used CRYSTAL06,[22] which uses Gaussian basis sets with periodic boundary conditions. All electronic band structure calculations used the DURAND_21G* basis sets[23] that replaces the 1s core basis functions using a pseudopotential.

This report provides useful and important guidelines for characterizing and designing CNT-based nanodevices, where we have shown that the band gaps of SWNTs obtained from the B3LYP hybrid density functional are in excellent agreement with experiment. Notably, B3LYP leads to accurate values of the small band gaps observed in the metallic zigzag (9,0), (12,0), and (15,0) SWNTs, whereas previous calculations using LDA, PBE, PW91, GW, and TB do not. Our results are significant for applications of SWNTs in nanoelectronics, where controlling whether the CNT is metallic or semiconducting is essential.

We also find that B3LYP accurately describes both the $\pi-\pi^*$ couplings and the $\sigma^*-\pi^*$ hybridizations.

Finally, we show that the band gaps and effective masses scale inversely proportional with the diameter squared for $d > 1.3$ nm.

DOI: 10.1021/jz100889u | J. Phys. Chem. Lett. 2010, 1, 2946–2950

SUPPORTING INFORMATION AVAILABLE

Geometries of optimized structures and additional band structures. This material is available free of charge via the Internet at http://pubs.acs.org.

AUTHOR INFORMATION

Corresponding Author:

*To whom correspondence should be addressed. Phone: (626) 395-2731. Fax: (626) 585-0918. E-mail: wag@wag.caltech.edu.

ACKNOWLEDGMENT This work was supported partially by Intel Components Research (Kevin O'Brien, Florian Gstrein, and James Blackwell), by the National Science Foundation (CCF-0524490 and CTS-0608889), and the Functional Engineered Nano Architects (FENA) via the Microelectronics Advanced Research Corporation (MARCO) with the prime award (2009-NT-2048) at UCLA (PI Kang Wang). The computer systems used in this research were provided by ARO-DURIP and ONR-DURIP.

REFERENCES

(1) Ouyang, M.; Huang, J.-H.; Cheung, C. L.; Lieber, C. M. Energy Gaps in "Metallic" Single-Walled Carbon Nanotubes. *Science* **2001,** *292*, 702–705.

(2) Miyake, T.; Saito, S. Band-gap formation in (*n*,0) single-walled carbon nanotubes (n = 9,12,15,18): A first-principles study. *Phys. Rev. B* **2005,** *72*, 073404.

(3) Sun, G.; Kürti, J.; Kertesz, M.; Baughman, R. H. Variations of the Geometries and Band Gaps of Single-Walled Carbon Nanotubes and the Effect of Charge Injection. *J. Phys. Chem. B.* **2003,** *107*, 6924–6931.

(4) Perry, J. K.; Tahir-Kheli, J.; Goddard, W. A. Antiferromagnetic band structure of La_2CuO_4: Becke-3-Lee-Yang-Parr calculations. *Phys. Rev. B* **2001,** *63*, 144510.

(5) (a) Becke, A. D. Density-Functional Thermochemistry. III. The Role of Exact Exchange. *J. Chem. Phys.* **1993,** *98*, 5648–5652. (b) Stephens, P. J.; Devlin, F. J.; Chabalowski, C. F.; Frisch, M. J. Ab Initio Calculation of Vibrational Absorption and Circular Dichroism Spectra Using Density Functional Force Fields. *J. Phys. Chem.* **1994,** *98*, 11623–11627.

(6) Muscat, J.; Wander, A.; Harrison, N. M. On the Prediction of Band Gaps from Hybrid Functional Theory. *Chem. Phys. Lett.* **2003,** *342*, 397–401.

(7) Xu, X.; Goddard, W. A., III. Peroxone Chemistry: Formation of H_2O_3 and Ring-$(HO_2)(HO_3)$ from O_3/H_2O_2. *Proc. Natl. Acad. Sci. U.S.A.* **2002,** *99*, 15308–15312.

(8) Xu, X.; Kua, J.; Periana, R. A.; Goddard, W. A., III. Structure, Bonding, And Stability of a Catalytica Platinum(II) Catalyst: A Computational Study. *Organometallics* **2003,** *22*, 2057–2068.

(9) Ashcroft, N. W.; Mermin, N. D. *Solid State Physics*; Holt, Rinehart, and Winston: New York, 1976.

(10) Roberts, R. A.; Walker, W. C. Optical Study of the Electronic Structure of Diamond. *Phys. Rev.* **1967,** *161*, 730–735.

(11) Marchand, D.; Frétigny, C.; Laguës, M.; Batallan, F.; Simon, C.; Rosenman, I.; Pinchaux, R. Three-Dimensional Band Structure of Graphite Studied by Angle-Resolved Photoemission Using Ultraviolet Synchrotron Radiation. *Phys. Rev. B* **1984,** *30*, 4788–4795.

(12) Cohen, A. J.; Mori-Sanchez, P.; Yang, W. Fractional Charge Perspective on the Band Gap in Density-Functional Theory. *Phys. Rev. B* **2008,** *77*, 115123.

(13) Matsuda, Y.; Deng, W.-Q.; Goddard, W. A., III. Contact Resistance Properties between Nanotubes and Various Metals from Quantum Mechanics. *J. Phys. Chem. C* **2007,** *111*, 11113–11116.

(14) Barone, V.; Peralta, J. E.; Wert, M.; Heyd, J.; Scuseria, G. E. Density Functional Theory Study of Optical Transitions in Semiconducting Single-Walled Carbon Nanotubes. *Nano Lett.* **2005,** *5*, 1621–1624.

(15) Blase, X.; Benedict, L. X.; Shirley, E. L.; Louie, S. G. Hybridization Effects and Metallicity in Small Radius Carbon Nanotubes. *Phys. Rev. Lett.* **1994,** *72*, 1878–1881.

(16) Saito, R.; Fujita, M.; Dresselhaus., G.; Dresselhaus, M. S. Electronic-Structure of Chiral Graphene Tubules. *Appl. Phys. Lett.* **1992,** *60*, 2204–2206.

(17) Cao, J. X.; Yan, X. H.; Ding, J. W.; Wang., D. L. Band Structures of Carbon Nanotubes: The sp^3s^* Tight-Binding Model. *J. Phys.: Condens. Matter* **2001,** *13*, L271–L275.

(18) Wildöer, J. W. G.; Venema, L. C.; Rinzler, A. G.; Smalley, R. E.; Dekker, C. Electronic Structure of Atomically Resolved Carbon Nanotubes. *Nature* **1998,** *391*, 59–62.

(19) Guo, Y.; Karasawa, N.; Goddard, W. A., III. Prediction of Fullerene Packing in C_{60} and C_{70} Crystals. *Nature* **1991,** *351*, 464–467.

(20) Gao, G.; Çağin, T.; Goddard, W. A., III. Position of K Atoms in Doped Single-Walled Carbon Nanotube Crystals. *Phys. Rev. Lett.* **1998,** *80*, 5556–5559.

(21) Chen, G.; Guo, Y.; Karsawa, N.; Goddard, W. A., III. Electron–Phonon Interactions and Superconductivity in K_3C_{60}. *Phys. Rev. B* **1993,** *48*, 13959–13970.

(22) Dovesi, R.; Saunders, V. R.; Roetti, C.; Orlando, R.; Zicovich-Wilson, C. M.; Pascale, F.; Civalleri, B.; Doll, K.; Harrison, N. M.; et al. *CRYSTAL 06 User's Manual*; University of Torino: Torino, Italy, 2006; see: http://www.crystal.unito.it.

(23) Causa, M.; Dovesi, R; Roetti, C. Pseudopotential Hartree–Fock Study of Seventeen III–V and IV–IV Semiconductors. *Phys. Rev. B* **1991,** *43*, 11937–11943.